Electronic Supporting Information (ESI)

Solution-Processed Multilayer Green Electrophosphorescent Devices with Self-Host Iridium Dendrimer as Nondoped Emitting Layer: Achieving High Efficiency while Avoiding Redissolution-Induced Batch-to-Batch Variation

Shumeng Wang, Baohua Zhang, Yang Wang, Junqiao Ding*, Zhiyuan Xie and Lixiang Wang*

State Key Laboratory of Polymer Physics and Chemistry
Changchun Institute of Applied Chemistry, Chinese Academy of Sciences
Changchun 130022 (P. R. China)
E-mail: junqiaod@ciac.ac.cn; lixiang@ciac.ac.cn

Experimental Section

Materials: PEDOT:PSS (Clevios P CH8000) was purchased from Heraeus Precious Metals GmbH Co. KG. Liq was purchased from Luminescence Technology Corp. G0, G1, G2, B-G2 and SPPO13 were synthesized in our laboratory according to the literature methods.[1-3]

Solvent resistance test: UV-Vis absorption spectra before and after alcohol spin-rinsing for the dendrimer films on quartz substrate were measured using Perkin-Elmer Lambda 35 UV-Vis spectrometer at room temperature. The nomalized remaining thickness is calculated from the ratio of integrated intensity of UV-Vis absorption spectra after alcohol spin-rinsing to the value before alcohol spin-rinsing. AFM measurements for dendrimer films before and after alcohol spin-rinsing were carried out using Veeco Instruments in the tapping mode with a 2 N m^{-1} probe in the atmospheric environment. All the AFM samples was prepared above PEDOT:PSS substrate and the forming condition is the same to the device preparation below.

Device preparation and characterization: All-solution-processed multilayer nondoped PhOLEDs were prepared with a structure of ITO/PEDOT:PSS (50 nm)/EML (30 nm)/SPPO13 (55 nm)/Liq (1 nm)/Al (100 nm). Dispersion of PEDOT:PSS in water was spin-coated onto the cleaned and UV-violet-ozone (UVO) treated ITO substrates. After baked at 120 ^{o}C for 30 min in air condition, the self-host dendrimers were spin-coated onto PEDOT:PSS from their chlorobenzene solutions at a concentration of 10 mg ml^{-1} and annealed at 100 ^{o}C for 30 min under nitrogen to form the EML. Subsequently, the electron-transporting material SPPO13 was spin-coated onto the EML from its isobutanol solution at a concentration of 10 mg ml^{-1} and then annealed at 60 ^{o}C for 30 min under nitrogen to form ETL. Finally, the cathode containing a 1-nm-thick Liq interfacial layer and a 100-nm-thick Al layer was deposited using thermal evaporation at a pressure under 4×10^{-4} Pa. All the measurements were carried out at room temperature in air conditions. The current density-voltage-luminance (*J-V-L*) characteristics were measured using a Keithley source measurement unit (calibrated silicon photodiode, Keithley 2400 and Keithley

2000), and the EL spectra were measured using CS2000A spectroscan photometer. The EQE was calculated from the luminance, current density and EL spectra assuming a Lambertian distribution.

References:

1 K. S. Yook, S. E. Jang, S. O. Jeon, J. Y. Lee, *Adv. Mater.* 2010, **22**, 4479.

2 J. Ding, J. Gao, Y. Cheng, Z. Xie, L. Wang, D. Ma, X. Jing, F. Wang, *Adv. Funct. Mater.* 2006, **16**, 575.

3 D. Xia, B. Wang, B. Chen, S. Wang, B. Zhang, J. Ding, L. Wang, X. Jing, F. Wang, *Angew. Chem., Int. Ed.* 2014, **53**, 1048.

4 N. Aizawa, Y.-J. Pu, M. Watanabe, T. Chiba, K. Ideta, N. Toyota, M. Igarashi, Y. Suzuri, H. Sasabe, J. Kido, *Nat. Commun.* 2014, **5**, 5756.

5 J. Park, C. Lee, J. Jung, H. Kang, K.-H. Kim, B. Ma, B. J. Kim, *Adv. Funct. Mater.* 2014, **24**, 7588.

6 T. Earmme, S. A. Jenekhe, *J. Mater. Chem.* 2012, **22**, 4660.

7 X. Yang, D. C. Müller, D. Neher, K. Meerholz, *Adv. Mater.* 2006, **18**, 948.

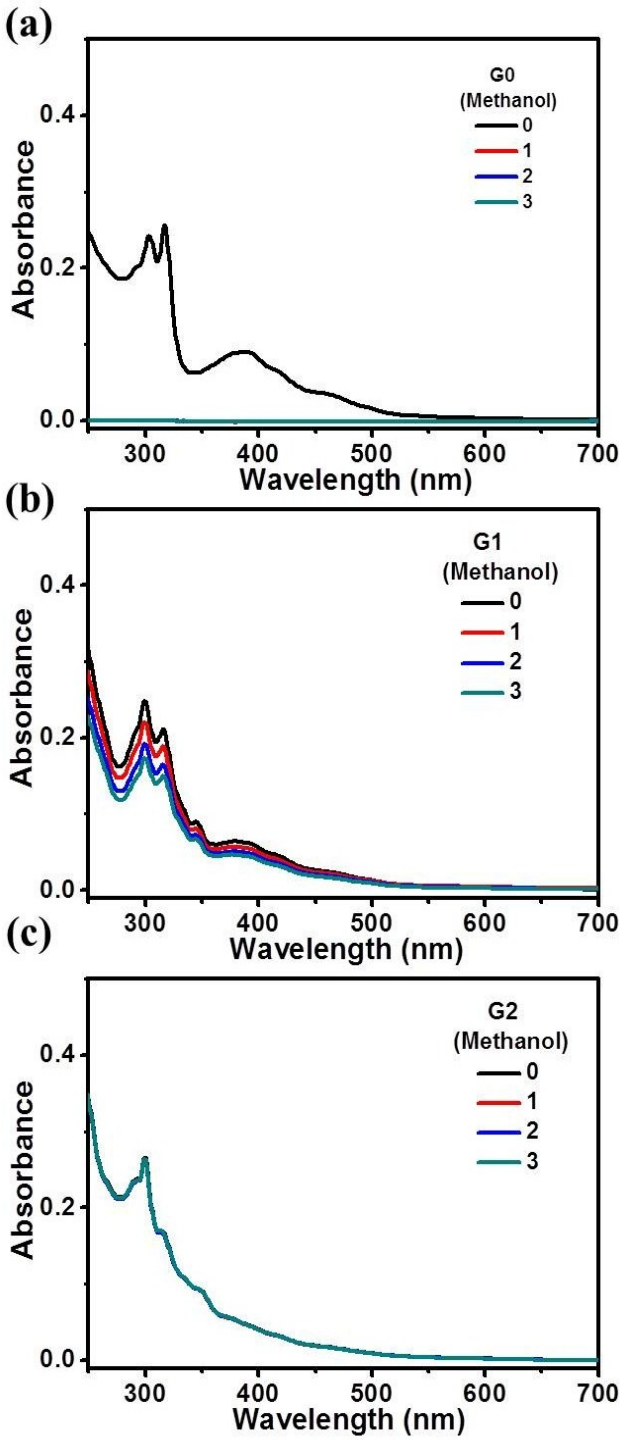

Fig. S1 UV-Vis absorption spectra for G0, G1 and G2 films after different spin-rinsing time by methanol.

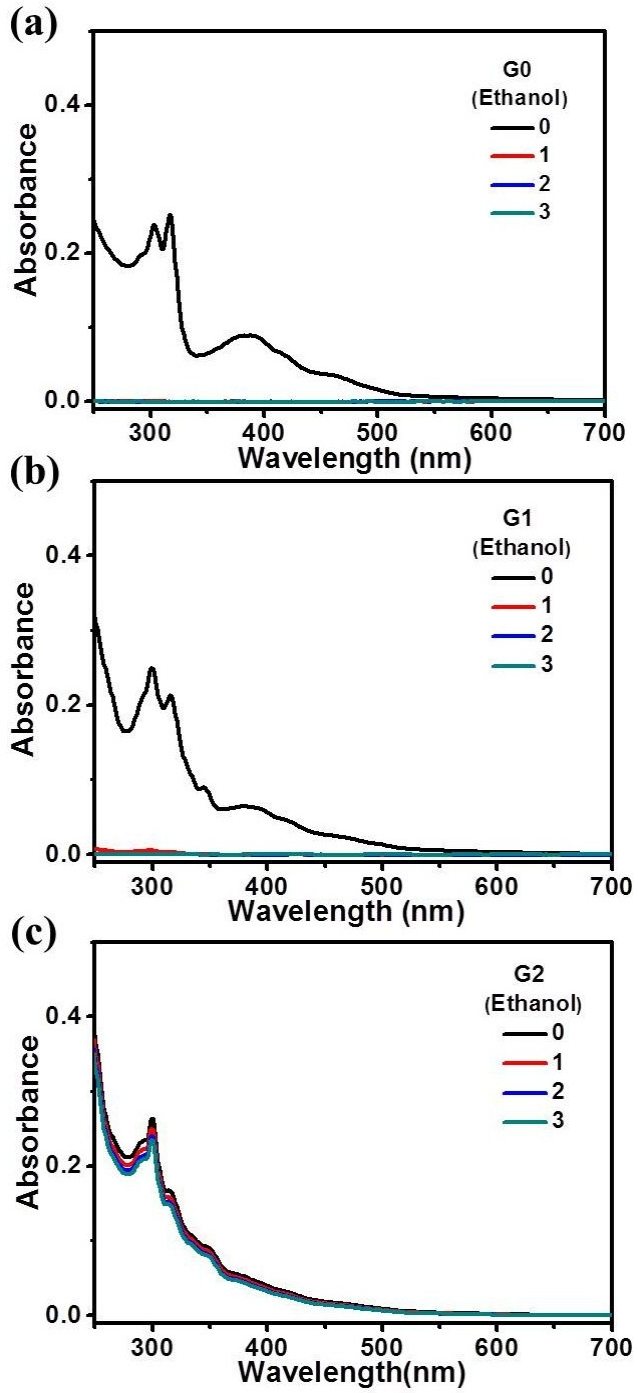

Fig. S2 UV-Vis absorption spectra for G0, G1 and G2 films after different spin-rinsing time by ethanol.

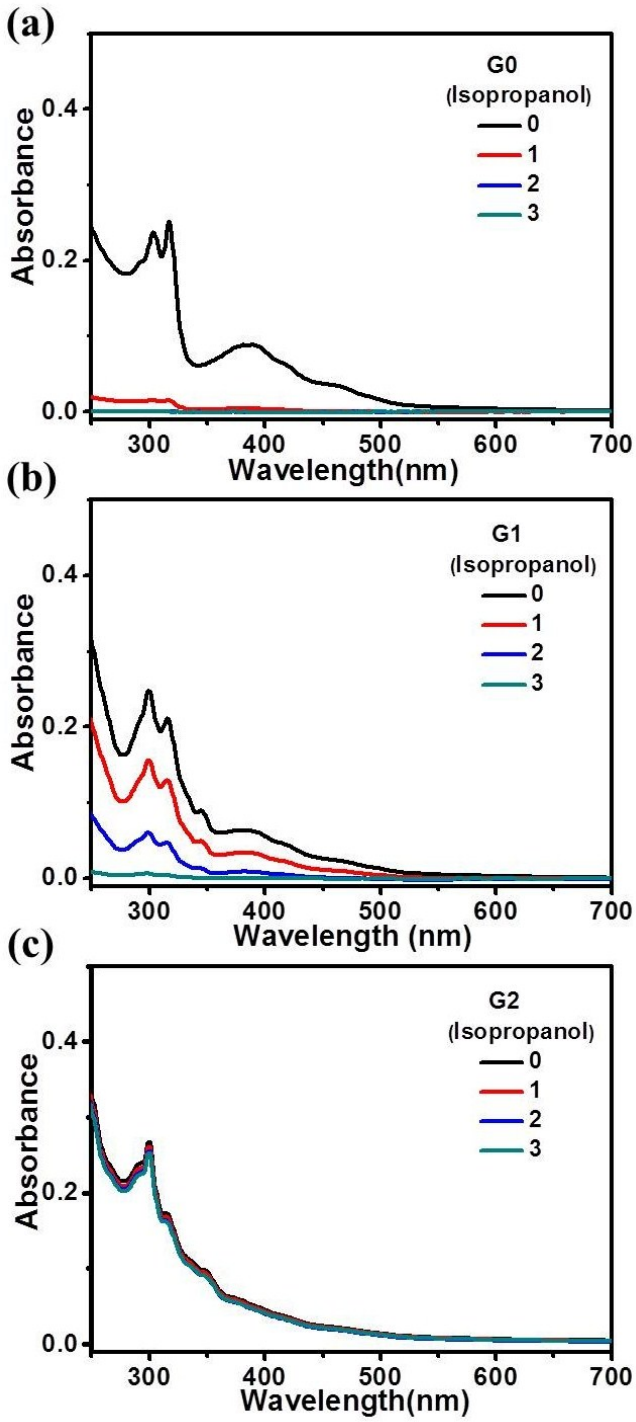

Fig. S3 UV-Vis absorption spectra for G0, G1 and G2 films after different spin-rinsing time by isopropanol.

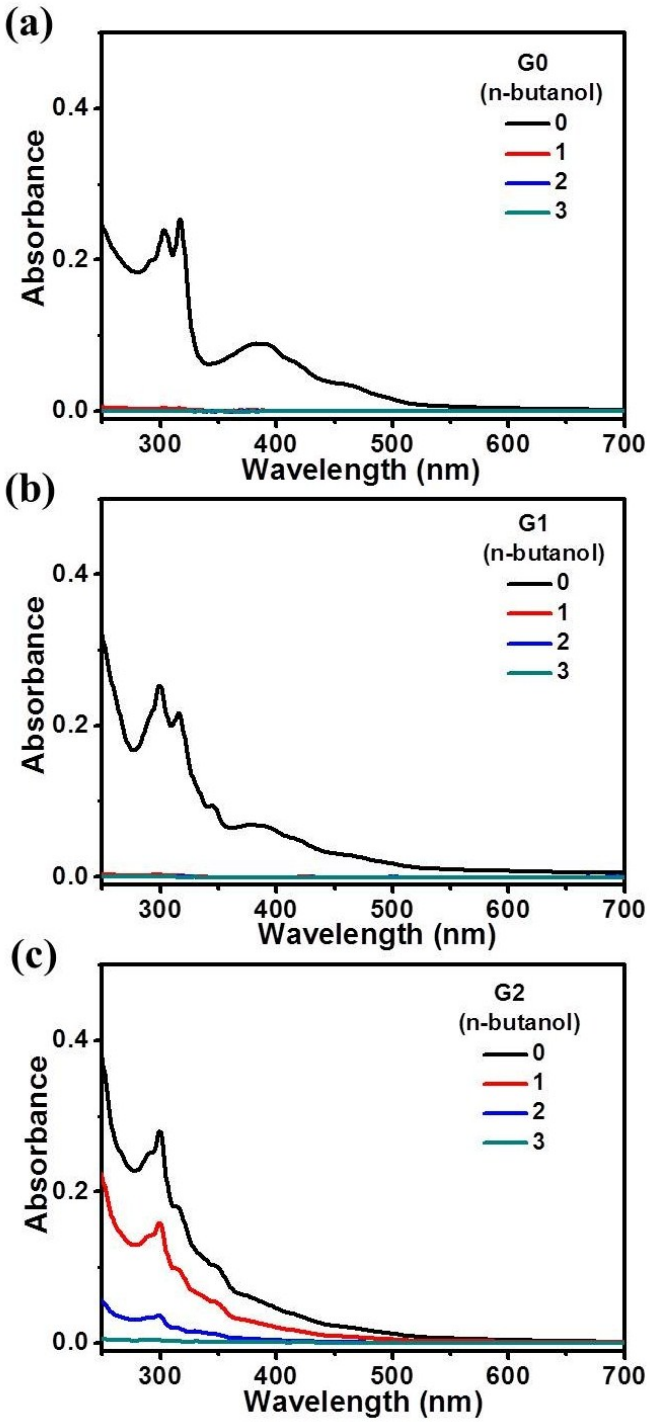

Fig. S4 UV-Vis absorption spectra for G0, G1 and G2 films after different spin-rinsing time by n-butanol.

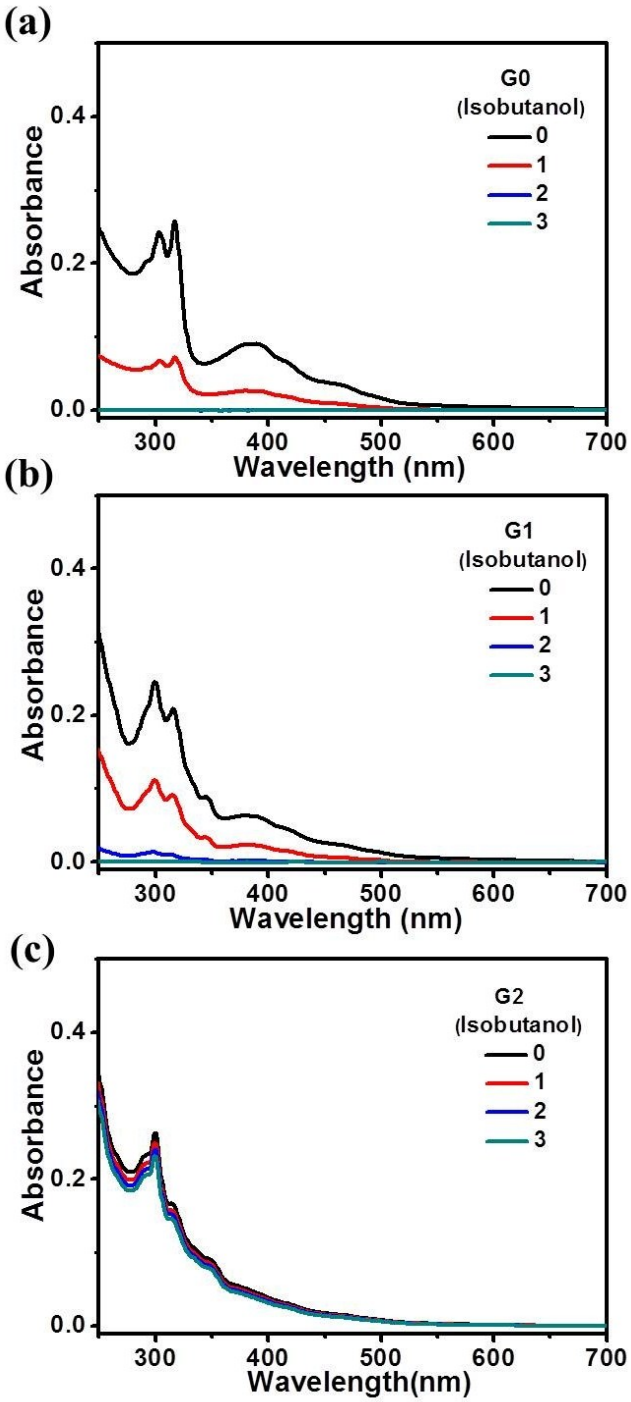

Fig. S5 UV-Vis absorption spectra for G0, G1 and G2 films after different spin-rinsing time by isobutanol.

Table S1 Comparison of the boiling point and viscosity for different alcohols.

Solvent	Methanol	Ethanol	Isopropanol	n-butanol	Isobutanol
Boiling point (^{o}C)	64.7	78.3	82.5	117.7	107
Viscosity (mPa·S)	0.59	1.41	2.43	2.95	3.95

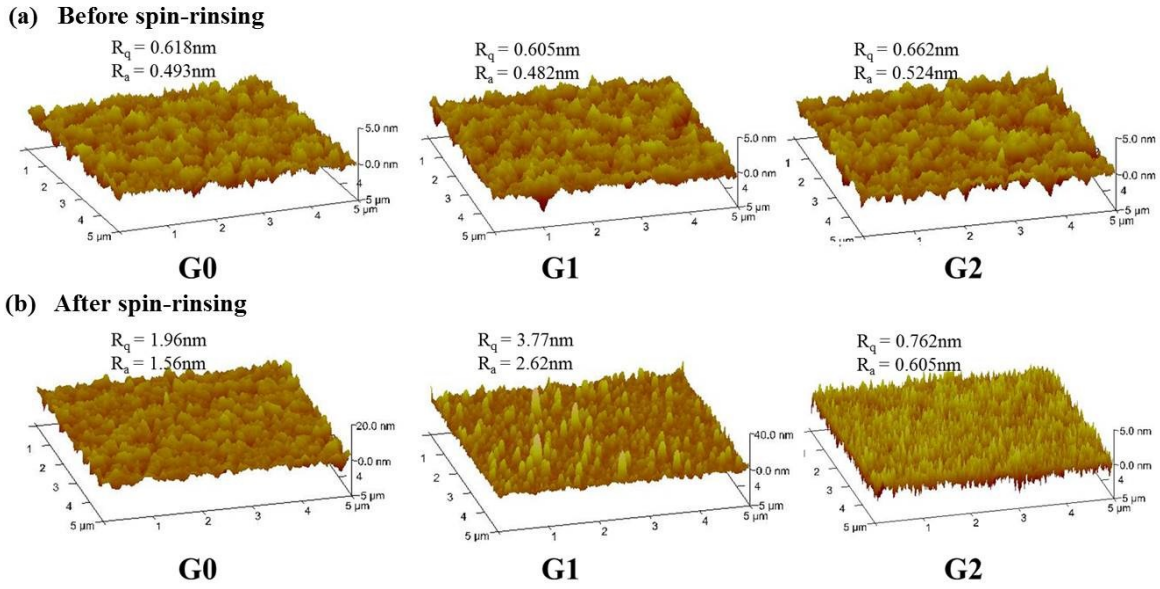

Fig. S6 AFM images of G0, G1 and G2 films before (a) and after (b) spin-rinsing with isobutanol.

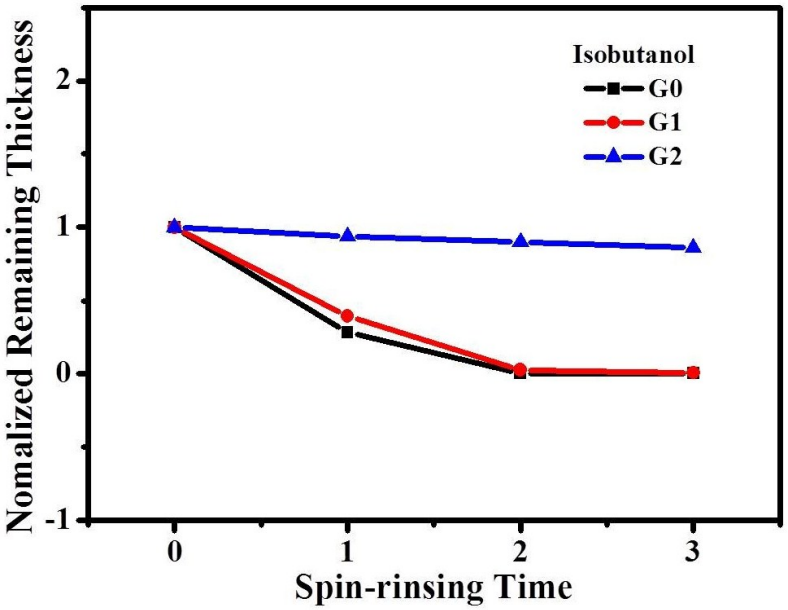

Fig. S7 Normalized remaining thickness of G0, G1 and G2 films as a function of isobutanol spin-rinsing time.

Table S2 Summary of the solution-processed multilayer device performance for self-host Ir dendrimers.

Device	V_{on} (V)	Max performance			Performance at 100/ 1000 cd m^{-2}				
		LE (cd A^{-1})	PE (lm W^{-1})	EQE (%)	V_d (V)	LE (cd A^{-1})	PE (lm W^{-1})	EQE (%)	CIE (x, y)
G2 (device-A)	2.6	68.4	69.4	21.2	3.7/5.0	68.4/64.5	58.1/40.5	21.2/19.9	(0.42, 0.56)
G2 (device-B)	2.6	52.2	53.3	15.7	3.6/4.9	52.2/49.0	45.5/31.4	15.7/14.8	(0.42, 0.56)

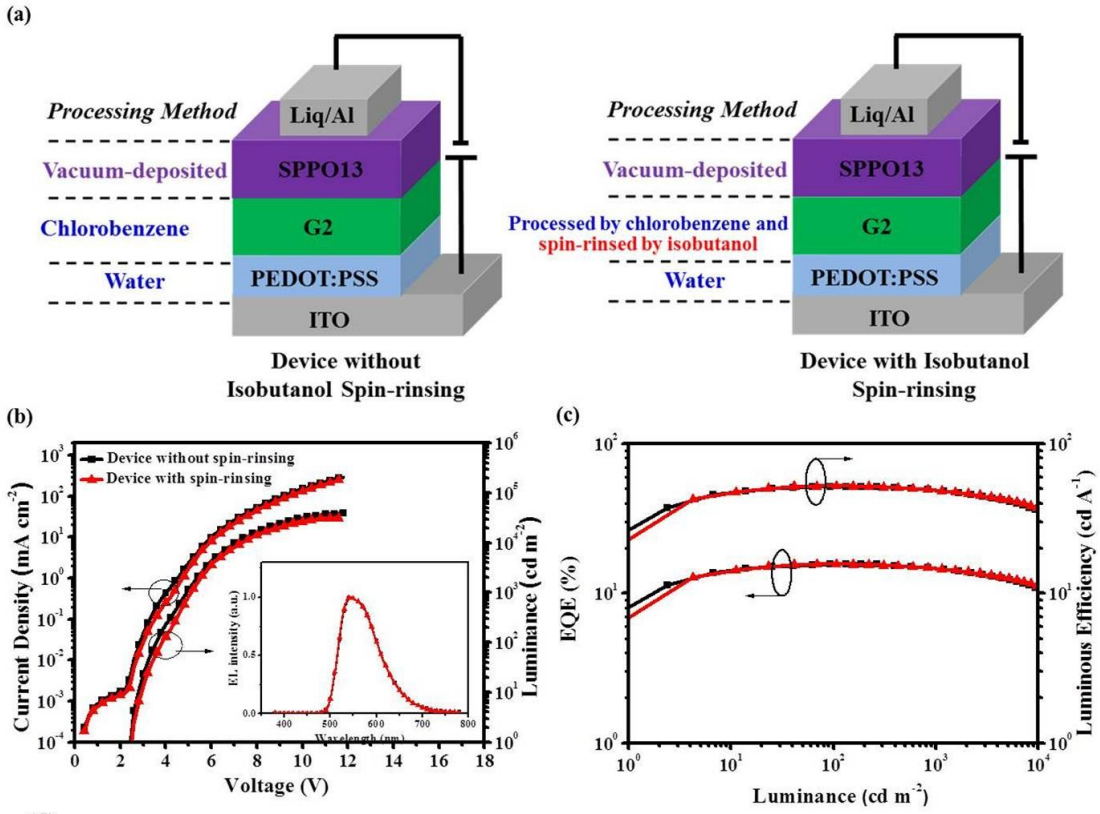

(d)

Device	V_{on} (V)	Max performance			Performance at 100/1000 cd m^{-2}				
		LE (cd A^{-1})	PE (lm W^{-1})	EQE (%)	V_d (V)	LE (cd A^{-1})	PE (lm W^{-1})	EQE (%)	CIE (x,y)
without spin-rinsing	2.6	52.2	53.3	15.7	3.6/4.9	52.2/49.0	45.5/31.4	15.7/14.8	(0.42, 0.56)
with spin-rinsing	2.6	52.0	51.0	15.7	3.8/5.1	52.0/48.8	42.9/30.1	15.6/14.7	(0.42, 0.56)

Fig. S8 Effect of isobutanol spin-ring on the emitting layer: (a) Device structures and fabricating conditions; (b) Current density-voltage-luminance (*J-V-L*) characteristics. Inset: EL spectra; (c) EQE and luminous efficiency as a function of luminance; (d) Table of device performance.

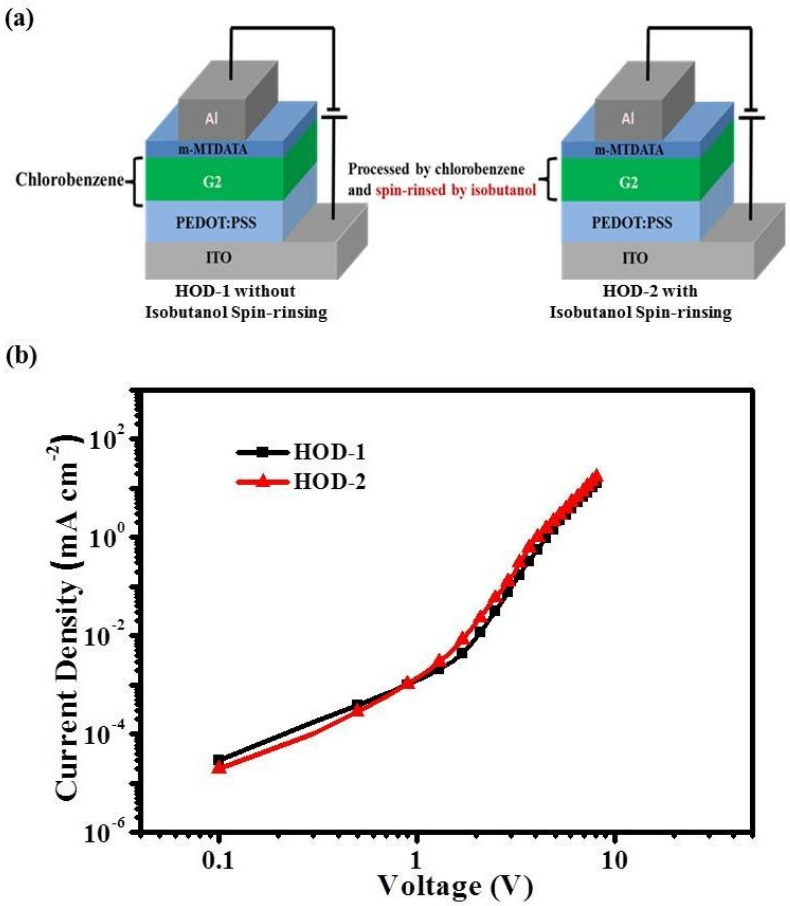

Fig. S9 Comparison between hole-only devices without and with isobutanol spin-rinsing: (a) Device structures and fabricating conditions; (b) Voltage dependence of the current density.

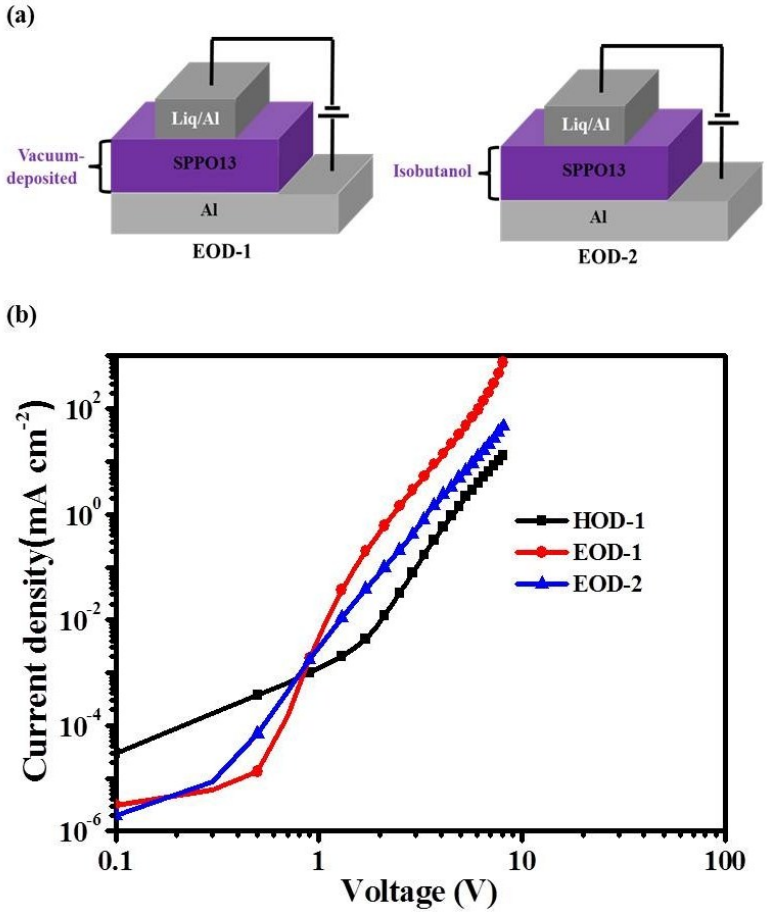

Fig. S10 Comparison between electron-only devices with vacuum-deposited and solution-processed SPPO13 layer: (a) Device structures and fabricating conditions; (b) Voltage dependence of the current density.

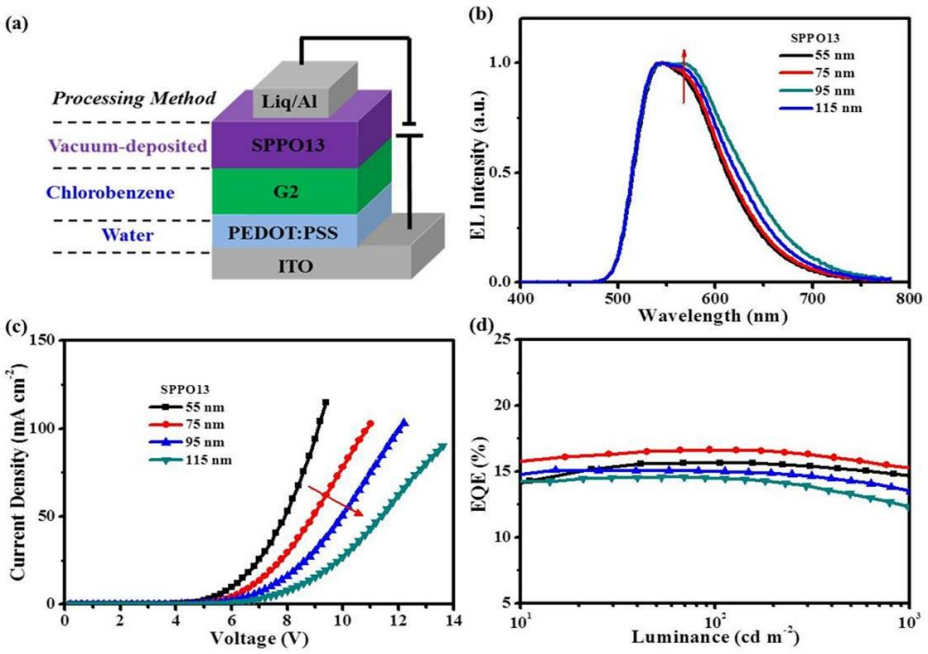

(e)

SPPO13 (nm)	V_{on} (V)	Max performance			Performance at 100/1000 cd m^{-2}				
		LE (cd A^{-1})	PE (lm W^{-1})	EQE (%)	V_d (V)	LE (cd A^{-1})	PE (lm W^{-1})	EQE (%)	CIE (x, y)
55	2.6	52.2	53.3	15.7	3.6/4.9	52.2/49.0	45.5/31.4	15.7/14.8	(0.42, 0.56)
75	2.7	55.3	55.3	16.6	4.0/5.6	55.3/50.6	43.4/28.4	16.6/15.2	(0.43, 0.56)
95	2.7	48.4	50.2	15.1	4.2/6.0	48.2/43.4	36.0/22.7	15.0/13.5	(0.44, 0.55)
115	2.8	44.5	45.1	14.6	5.0/6.8	44.2/37.6	27.7/17.4	14.5/12.3	(0.45, 0.54)

Fig. S11 Dependence of the ETL thickness on the performance of device B: (a) Device structures and fabricating conditions; (b) EL spectra; (d) Current density-voltage curves; (d) EQE as a function of luminance; (e) Table of device performance. As one can see, when the thickness of the vacuum-deposited SPPO13 layer is up from 55 nm to 75 nm, the EQE is increased from 15.7% to 16.6%. This demonstrates the contribution from charge balance caused by the reduction of electron flux, which is consistent with the case observed in device A. However, when it is further up from 75 nm to 115 nm, the EQE is reduced from 16.6% to 14.6%. In this case, the exciton formation zone is far away from the cathode, and the microcavity effect may play an important role on the device performance. This is further verified by the EL spectra, where the emission from the shoulder is gradually enhanced with the increasing thickness of SPPO13.

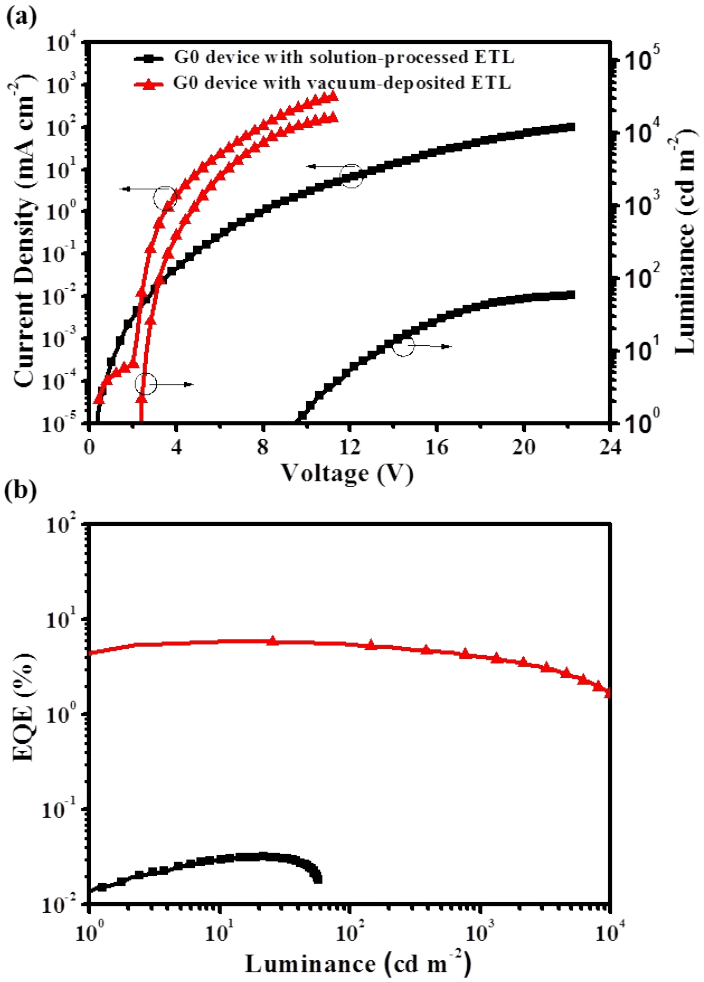

Fig. S12 Comparison between G0-based devices with vacuum-deposited and solution-processed ETL: (a) Current density-voltage-luminance (*J*-*V*-*L*) characteristics; (b) EQE as a function of luminance.

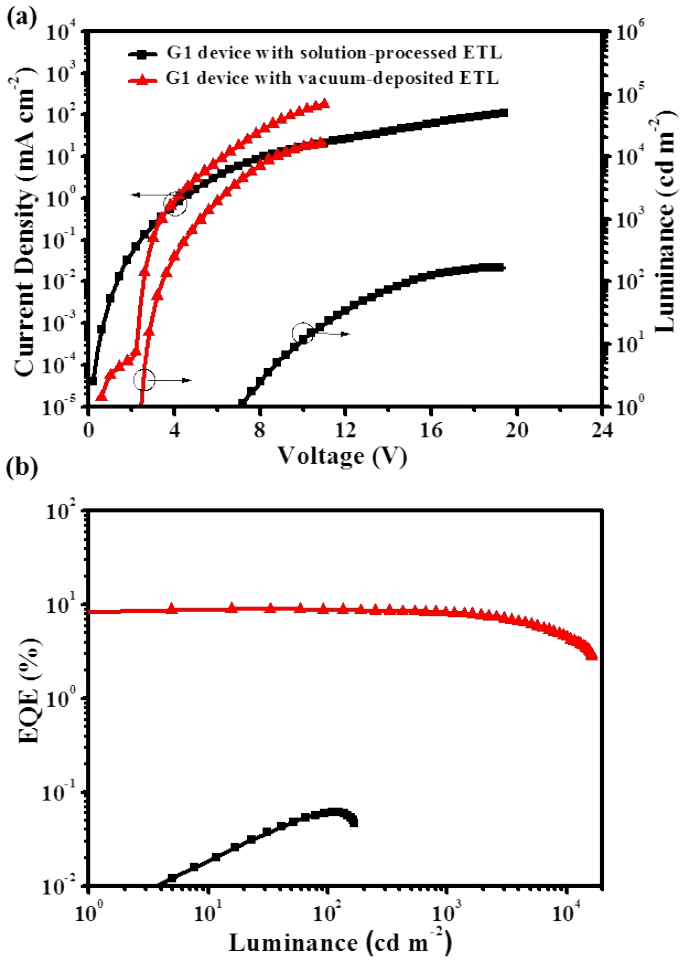

Fig. S13 Comparison between G1-based devices with vacuum-deposited and solution-processed ETL: (a) Current density-voltage-luminance (*J*-*V*-*L*) characteristics; (b) EQE as a function of luminance.

Table S3 Summary of the device performance for G0 and G1.

Device	V_{on} (V)	Max performance		
		LE (cdA^{-1})	PE (lmW^{-1})	EQE (%)
[a]G0	9.5	0.10	0.02	0.03
[b]G0	2.4	19.4	23.4	5.9
[a]G1	7.1	0.20	0.04	0.06
[b]G1	2.6	29.1	35.6	9.0

[a]Devices with a solution-processed ETL; [b]Devices with a vacuum-deposited ETL.

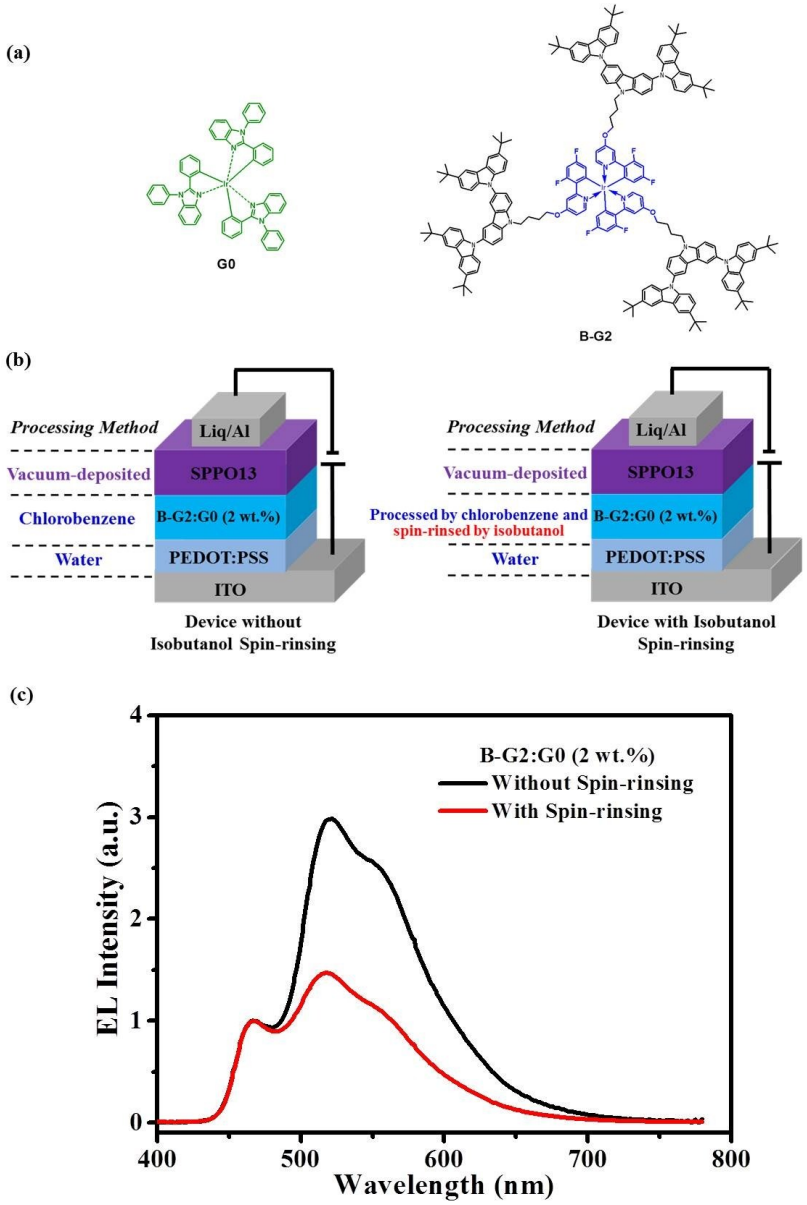

Fig. S14 Investigation of redissolution of small molecular phosphors in doped system by mixing 2 wt. % G0 with self-host blue Ir dendrimer B-G2. Here B-G2 is used as the matrix because it not only has excellent alcohol resistance, but also emits blue light that can act as an internal standard to calibrate the intensity of green emission from G0. (a) Molecular structures of G0 and B-G2; (b) Device structures and fabricating conditions; (c) EL spectra where the 468 nm emission from B-G2 is normalized.

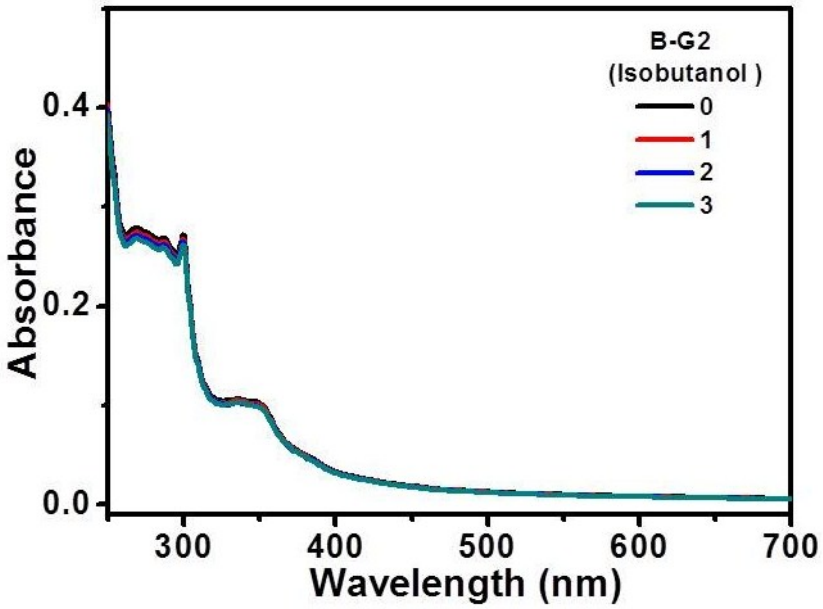

Fig. S15 Good alcohol resistance of self-host blue Ir dendrimer B-G2: UV-Vis absorption spectra for B-G2 film after different time spin-rinsing by isobutanol.

Table S4 Performance comparison of solution-processed multilayer green PhOLEDs.

Device Configuration	Voltage (V)	EQE (%)	Ref
	V_{on}/100/1000 cdm^{-2}	Max/100/1000 cdm^{-2}	
Nondoped	2.6/3.7/5.0	21.2/21.2/19.9	This work
Doped	--/4.8/6.3	--/22/20	4
Doped	--/--/--	11.8/--/--	5
Doped	5.8/--/--	16.1/--/--	6
Doped	--/--/--	18.8/18.8/15.7	7